Environmental Science & Technology

pubs.acs.org/est

Article

Ethylene Oxide in Southeastern Louisiana's Petrochemical Corridor: High Spatial Resolution Mobile Monitoring during HAP-MAP

Ellis S. Robinson, Mina W. Tehrani, Amira Yassine, Shivang Agarwal, Benjamin A. Nault, Carolyn Gigot, Andrea A. Chiger, Sara N. Lupolt, Conner Daube, Anita M. Avery, Megan S. Claflin, Harald Stark, Elizabeth M. Lunny, Joseph R. Roscioli, Scott C. Herndon, Kai Skog, Jonathan Bent, Kirsten Koehler, Ana M. Rule, Thomas Burke, Tara I. Yacovitch, Keeve Nachman, and Peter F. DeCarlo*

Cite This: https://doi.org/10.1021/acs.est.3c10579

Read Online

ACCESS | Metrics & More | Article Recommendations | Supporting Information

ABSTRACT: Ethylene oxide ("EtO") is an industrially made volatile organic compound and a known human carcinogen. There are few reliable reports of ambient EtO concentrations around production and end-use facilities, however, despite major exposure concerns. We present *in situ*, fast (1 Hz), sensitive EtO measurements made during February 2023 across the southeastern Louisiana industrial corridor. We aggregated mobile data at 500 m spatial resolution and reported average mixing ratios for 75 km of the corridor. Mean and median aggregated values were 31.4 and 23.3 ppt, respectively, and a majority (75%) of 500 m grid cells were above 10.9 ppt, the lifetime exposure concentration corresponding to 100-in-one million excess cancer risk (1×10^{-4}). A small subset (3.3%) were above 109 ppt (1000-in-one million cancer risk, 1×10^{-3}); these tended to be near EtO-emitting facilities, though we observed plumes over 10 km from the nearest facilities. Many plumes were highly correlated with other measured gases, indicating potential emission sources, and a subset was measured simultaneously with a second commercial analyzer, showing good agreement. We estimated EtO for 13 census tracts, all of which were higher than EPA estimates (median difference of 21.3 ppt). Our findings provide important information about EtO concentrations and potential exposure risks in a key industrial region and advance the application of EtO analytical methods for ambient sampling and mobile monitoring for air toxics.

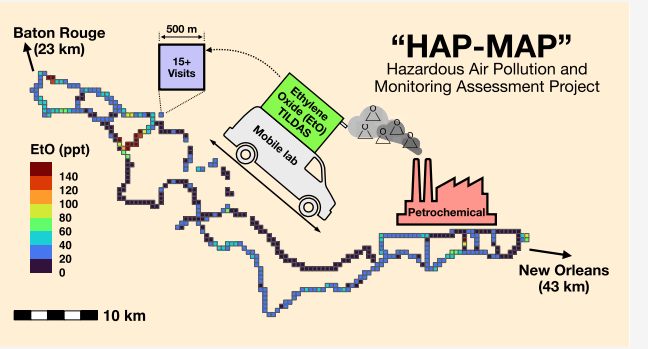

KEYWORDS: *ethylene oxide, industrial emissions, hazardous air pollutants (HAPs), air pollution, mobile monitoring, optical spectroscopy, environmental health, Louisiana, cancer risk*

1. INTRODUCTION

Ethylene oxide ("EtO," chemical formula: C_2H_4O) is a volatile organic compound (VOC) used as a petrochemical feedstock for commercial chemicals (e.g., ethylene glycols) as well as a sterilizing and fumigating agent for medical equipment and food safety. It is most commonly produced by the catalytic direct oxidation of ethylene.[1] EtO is also hazardous to human health, with inhalation being the primary route of exposure. While acute effects exist for high levels of EtO, health concerns revolve around chronic effects, as EtO is a known human carcinogen associated with a variety of cancers (leukemia, myeloma, lymphoma, and breast cancer) and is also considered mutagenic.[2] EtO is extremely carcinogenic relative to other common hazardous VOCs, and so even low levels of chronic EtO exposure pose substantial risks: the chronic EtO exposure concentration that corresponds to the upper limit of EPA's acceptable cancer risk range, 100-in-one million elevated cancer risk (1×10^{-4}), is 10.9 ppt. The cancer potency of EtO and how it should be regulated are currently hotly contested, both in courts and in the public square: industry groups dispute the accuracy of EtO's toxicity,[3] while environmental advocates think that EtO regulations need to be even tighter.[4,5]

Despite growing concern over these environmental health issues, there are few reports of ambient EtO measurements. Roughly 20% of total U.S. EtO emissions are thought to come from sterilization and fumigation operations,[6] and most reports of near-source ambient EtO have been conducted around these facilities.[7−13] These emissions fit into the category of EtO end-use and are sometimes located near population centers.[14] The

Received: December 19, 2023
Revised: May 3, 2024
Accepted: May 3, 2024

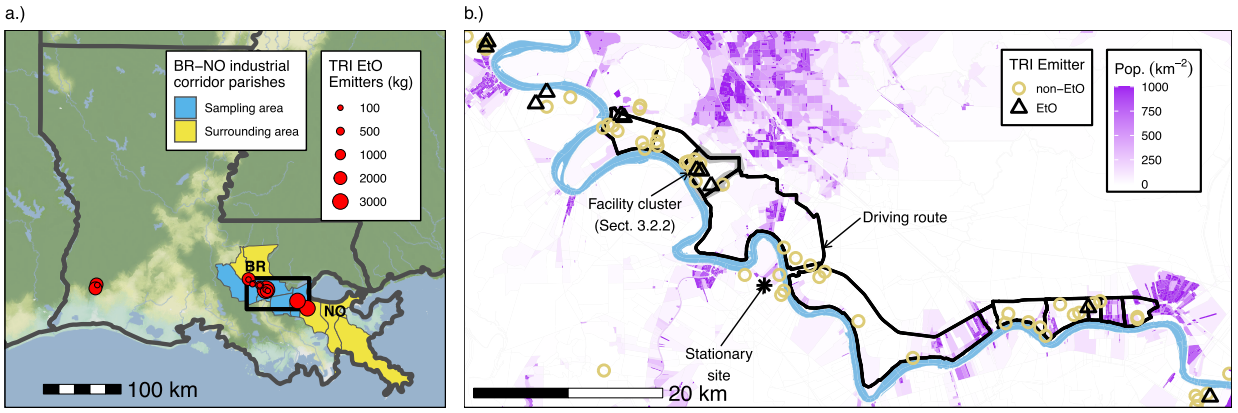

Figure 1. Overview maps illustrating the context for this measurement campaign. (a) Map of state of Louisiana, highlighting the Baton Rouge (BR)-New Orleans (NO) Mississippi River industrial corridor and the locations and relative magnitudes of EtO emission sources (per 2022 Toxics Release Inventory (TRI) annual emissions). We defined the larger industrial corridor by parish boundaries for those between BR and NO along the MS River. Parishes are colored according to whether we made measurements within them or not. The black box shows the spatial extent of the map in the left panel of the sampling domain. (b) Map of the sampling area, highlighting the AML driving route, population density in the surrounding areas (from 2020 Census block-level estimates), location of the stationary site and facility cluster (described in more detail in Section 3.2.2), and TRI-listed facility locations. Population density information is meant to highlight the locations of communities living near the industrial fenceline.

majority of total EtO emissions (~75%), however, are thought to come from petrochemical manufacturing,[6] though comparatively fewer reports of ambient EtO exist around these production and processing facilities.[15] A significant fraction (~15−36%) of emissions from petrochemical manufacturing are self-reported as nonstack, "fugitive" emissions from, e.g., pump, valve, or pipeline leaks.[6] Nonoccupational human exposure to EtO is likely highest for people who live at or near the fenceline of EtO production, processing, or end-use facilities.[16]

A number of the largest EtO emitters in the U.S. are located in southeastern Louisiana, which contains a high density of the country's petrochemical manufacturing facility fleet. A majority (~68%) of the total hazard from industrial facility air emissions in this region is attributable to EtO (discussed further in Section 3.1). As such, there has been significant recent concern over EtO exposure in the industrial corridor between Baton Rouge and New Orleans, exemplified by the recent legal battle between environmental advocates and Formosa Plastics over the siting of a new plant in St. James Parish that would be permitted to release EtO.[17] These concerns are part of a broader history of environmental justice and health concerns among residents and advocates within the region, illustrated by a colloquial nickname for the area, "Cancer Alley".[18] Indeed, there are higher cancer incidence rates within the region, which have been connected to industrial air pollution and shown to fall disproportionately on impoverished and black neighborhoods.[19] Notably, there have been no published measurements of EtO in this area.

One reason for the relative dearth of reported ambient EtO concentrations in general is that measurement is an analytical challenge. Traditionally, ambient EtO is quantified by collecting air samples in steel canisters for off-line analysis using paired gas chromatography−mass spectrometry (GC−MS).[20] Occupational exposure has been assessed using passive dosimeter badges, though the limit of detection of this method (>20 ppb[21]) is far higher than most reported ambient EtO measurements. These methods are relatively expensive, fail to capture short temporal variations and pose logistical challenges for capturing spatial variations. Additionally, both the EPA[22] and Hoisington and Herrington[23] have demonstrated that humidity and canister material can both influence in-canister EtO formation ("EtO growth") over days-long timeframes, complicating the interpretation of previously published EtO measurements from canister sampling. A recent study from Mei et al.[9] showed no correlation at all between canister sampling and a real-time spectroscopic EtO instrument over a months-long colocation. Even before considering in-canister growth, spatiotemporal variability makes offline canister sampling not ideal for characterizing EtO emission sources and understanding their impacts on human populations.

The landscape for assessing ambient EtO levels, however, is changing. Several *in situ* optical instruments have been recently developed that enable EtO detection in real-time.[8,24,25] Most of these new techniques have sub-1 ppb precision at relatively short averaging periods (1 s to 1 h) and are increasingly being applied to measure EtO in both background and near-source environments.[7−9,15] Given that 100-in-one million elevated cancer risk corresponds to a lifetime exposure concentration of 10.9 ppt, high accuracy and precision measurements of EtO are needed to pinpoint risks posed to populations. The fast time-response of these instruments offers the possibility for assessing the spatial patterns of ambient EtO concentrations via mobile monitoring, a practice that is somewhat common for certain pollutants, particularly some criteria air pollutants and others related to traffic (see Wang et al.[26] and references therein), but is far less common for air toxics.[27,28]

We used two commercial optical instruments aboard mobile platforms to measure EtO across a portion of the petrochemical industrial corridor of southeastern Louisiana as part of the Hazardous Air Pollutant Monitoring and Assessment Project (HAP-MAP). From this data set, we present an analysis of EtO plumes and highly spatially resolved estimates of EtO mixing ratios across the region. From these EtO estimates, we perform a spatial analysis of EtO mixing ratios within different land-use categories based on proximity to industrial point sources, as well as a comparison of census tract-level EtO estimates between our mobile measurements and modeled mixing ratios from EPA's 2019 Air Toxics Screening Assessment ("AirToxScreen"[29]). These results are highly relevant to the communities within our study domain, as

https://doi.org/10.1021/acs.est.3c10579
Environ. Sci. Technol. XXXX, XXX, XXX−XXX

well as to the growing literature related to EtO measurements and impacts.

2. METHODS

The larger HAP-MAP project represents an effort to measure a wide suite of hazardous air pollutants, both gas- and particle-phase, at the fenceline of heavy industry and within adjacent communities with the ultimate goal of assessing exposure and related health risks. This paper presents EtO measurements from two different instruments, each aboard a different mobile platform as part of HAP-MAP. Mobile platforms enabled on-road EtO measurements across the sampling domain, which we use to assess spatial differences in EtO mixing ratios and to investigate EtO plumes emitted from different facilities. These measurements were conducted in winter 2023 over 23 separate drives that spanned 27 days (Jan. 31 to Feb. 26).

The southeastern Louisiana petrochemical industrial corridor stretches over 160 km along the Mississippi River, from areas north of Baton Rouge to areas south and east of New Orleans and contains 1.6 million people. We focused our measurements in the middle of the corridor, where the density of petrochemical facilities is highest. As shown in Figure 1a, the majority (12 of 15) of EtO-emitting facilities in Louisiana listed in the EPA's Toxics Release Inventory (TRI) are within the industrial corridor between Baton Rouge and New Orleans. The other three listed facilities are in or near Lake Charles in the western portion of the state. Most of the EtO-emitting facilities in the corridor are within or very close to our sampling area, which spanned parts of Iberville, Ascension, St. James, and St. John the Baptist Parishes (Louisiana is divided into parishes as other U.S. states are divided into counties). When not performing mobile sampling, instruments aboard the mobile lab continued ambient sampling while parked at a stationary site (coordinates: 30.0890, −90.9344) near Donaldsonville, LA (pop. ∼6700).

2.1. Measurements. An Aerodyne EtO tunable infrared laser direct absorption spectrometer (TILDAS) instrument[8] was onboard the Aerodyne Mobile Laboratory (AML), and a Picarro G2920 EtO cavity ringdown spectrometer (CRDS) instrument (Picarro, Inc.[24]) was onboard the Johns Hopkins University mobile laboratory (JHUML). The TILDAS instrument is the primary data source used for this analysis, though we present in-plume data from the CRDS in comparison with the TILDAS. We briefly describe each instrument and its operation below, with further details provided in the Supporting Information.

2.1.1. Ethylene Oxide–Aerodyne TILDAS. TILDAS is a fast (sub-1 Hz native response time) spectrometer that has been recently developed for EtO measurement in the 3065.7–3066.0 cm^{-1} region.[8] This region of the spectrum includes deep water lines as well as the absorption of other key species like C_2H_6, HCHO, C_2H_4, CH_4, and CH_3OH, all of which are accounted for with custom spectral fitting software ("TDLWintel," with spectroscopic details available in Yacovitch et al.[8]). Instrument detection limits (estimated as 3 × SD) are 186 ppt for 1s mobile data and 45 ppt for 100s stationary data. We estimate a 25% overall uncertainty for all measured EtO mixing ratios, due to uncertainties in gas standards and calibration error. See Supporting Information Methods section for more on TILDAS detection limits, instrument details, and calibration and zeroing.

The AML platform has been described extensively before;[28,30,31] it is a large step-utility van that hosts a variety of air pollutant and chemical measurements (see Figure S1). Further details about the AML inlets and other non-EtO instruments aboard the AML are provided in the Supporting Information.

2.1.2. Ethylene Oxide–Picarro CRDS. The Picarro EtO CRDS system (referred to as "CRDS" herein) aboard the JHUML was used for flexible, exploratory sampling to scout for plumes downwind of various facilities.

We also used the JHUML to perform vehicle chase drives behind the AML. Instrumentation onboard the JHUML was operated on battery power, and so we did not perform any nonmobile stationary sampling with the CRDS. Further details about the CRDS operation, inlet, and data quality, as well as details about the JHUML and vehicle chase drives, are presented in the Supporting Information.

2.1.3. Wind Speed and Direction. We measured wind direction (WD) and speed (WS) using two methods and used each data source depending on the circumstances. The AML has an on-board sonic anemometer (2D RMYoung Model 85004), which we use for analyzing wind data when the AML is at the stationary site. However, we found in-motion WD to be inaccurate, especially for low wind speeds, and so we do not use the on-board WD for pairing with mobile measurements. Instead, we use WD measured at a stationary site within the middle of the domain (coordinates: 30.0662, −90.8497) and assume it reflects wind behavior for the rest of the driving route. This wind measurement consisted of a QuantAQ MODULAIR-PM sensor paired with a sonic anemometer (Davis Instruments Model 6415), which records at 1 min intervals. Both anemometers have stated an accuracy of less than ±4 degrees."

2.2. Mobile Sampling Experimental Design. A major goal of this campaign was to provide spatially resolved average mixing ratios of EtO across the region to be used as the basis for risk analysis. Data collection by the AML was designed to meet this objective. We devised a sampling route that passed as many industrial sites as possible while also being manageable to drive in its entirety within a standard "shift" (∼8 h of driving). Over the course of a shift, we passed by most locations on the route once, though some sections of road had to be used multiple times in order to ensure full route coverage, and thus were passed more than once per driving shift (see Figure S2 for an illustration of example day's driving and Figure S3 for the four "sections" of the route we used for planning). We staggered departure from the stationary site and the order in which we drove route sections to minimize any bias that may arise from visiting a given location at the same time each day; we achieved fairly even data coverage across all hours of the day for our mobile sampling (see Figure S4).

As other previous mobile monitoring studies[32−34] have shown, repeatedly capturing measurements of an air pollutant at a location can provide representative concentrations for that location given a sufficient number of visits. Many factors influence the number of visits required for such an ensemble of measurements to paint a representative picture, including time of day, source strength at that location, pollutant type, and instrument noise, among others. We designed our sampling to capture 22 or more visits at each location and to be spread across times of day. Figure S5 shows the number of total unique visits within each grid cell for the full campaign.

2.3. Data Analysis. *2.3.1. Spatial Data Analysis.* To produce EtO mixing ratios resolved across space, we perform a reduction on the TILDAS data set that is conceptually similar

https://doi.org/10.1021/acs.est.3c10579
Environ. Sci. Technol. XXXX, XXX, XXX−XXX

to that described in Apte et al.[32] First, we spatially aggregate all of the raw 1 Hz measurements into 500 m grid cells. This cell size accommodated the fast road speeds of the AML (30−60 km/h, dictated by roads and traffic) while still providing high spatial resolution. We defined a grid cell "visit" to include all data points collected within a unique hour within that grid cell, and the "visit mean" as the mean of those within-hour data points. The overall grid cell values we report (e.g., Figure 6) are the mean of all visit means. This approach ensures that equal weights are given to each visit, as opposed to equal weights for each raw measurement, and thus reduces the bias that could arise from variability in how much time is spent in each grid cell for a given visit. We only report concentrations for grid cells that meet a minimum threshold requirement of 15 visits. The median number of 1 Hz data points collected per grid cell is 410 (250−721, 25th−75th percentiles, respectively).

We performed spatial aggregations related to proximity to facilities and census tracts as well. Grid cells were placed into one of three different categories: (1) within 1 km of a EtO-emitting facility, (2) within 1 km of a non-EtO-emitting facility, and (3) all other grid cells not within 1 km of any type of facility. We used 1 km of circular buffers around the coordinates of each facility and performed a spatial intersection with the grid cell centroids. Any grid cell intersecting the 1 km buffer of both an EtO emitter and a non-EtO emitter was put into the "within 1 km of an EtO emitter" category. We performed the above analysis using 1.5 and 2 km buffer sizes as well and present those results in the Supporting Information. Facility locations were represented as points by the coordinates listed in the TRI database.

To estimate census tract-level EtO mixing ratios, we assigned grid cells to the census tract containing the grid cell centroid. In the case of the census tract containing the stationary site, we use just the stationary site average EtO mixing ratio to estimate the tract average (see Supporting Information for full explanation). Tract-level EtO estimates are the mean of all within-tract grid cell estimates. We compare these to tract-level EtO estimates from 2019 AirToxScreen.

All spatial analysis was performed using the *sf: Simple Features for R* GIS library,[35] wind direction analysis was performed using the *openair* R package for air quality data analysis,[36] and maps were made using the *ggmap* R library.[37]

2.3.2. Plume Analysis. We used the TILDAS EtO time series (see Figure S6) to define, identify, and characterize plumes using a programmatic approach, which is conceptually similar to other work that has identified plumes from air pollutant concentration time series.[38,39] We defined plumes by any EtO measurements above a rolling mixing ratio threshold. This threshold was defined as three times the standard deviation (SD) above a rolling baseline, where the baseline is the 20th percentile (threshold = 3 × SD + 20th percentile.). We use a 20 min rolling window to calculate the baseline and threshold. Any EtO measurement above this threshold was defined as "plume" and below as "non-plume" (see Figure S7 for illustration). Consecutive "plume" data points were grouped together as a unique plume; if EtO concentrations fell below the threshold, then the next above-threshold data points would be the start of another, uniquely identified plume.

Within each plume, we also examined correlations between the time series of EtO and the mixing ratios of other gas-phase species measured aboard the AML. A full list of these auxiliary gas species measurements is described in the Supporting Information. For the purposes of this article, we use the time series of these other species for understanding the chemical mixture within EtO plumes. Within each EtO plume, we calculated the slope and R^2 value between EtO and each gas species, the plume duration (in time), the average and maximum EtO value, and the midpoint longitude and latitude. We used plume duration (in seconds) as opposed to spatial plume "width," which theoretically would be duration × driving speed, to filter select plumes that we present in Results. We do this because our characterization algorithm relies on the time series, and so duration is a more fundamental filtering quantity than "width" in terms of being able to discern signal from noise, as well as being able to include meaningful plumes that may have been detected while the AML was stationary or moving very slowly for whatever reason.

2.3.3. Stationary Site Analysis. During downtime from driving, the AML was parked in an RV lot ∼5 km east of Donaldsonville and connected to line power (generators off). We analyzed the TILDAS data collected at the stationary site to calculate summary statistics, identify any EtO diurnal pattern, and investigate EtO plumes with respect to wind direction.

2.3.4. RSEI and TRI Data Analysis. The EPA's Risk-Screening Environmental Indicators (RSEI) model[40] and the Toxic Release Inventory (TRI),[6] while imperfect, provided valuable information for sampling route planning as well as understanding the overall scope of EtO emissions and their associated hazards in southeastern Louisiana. TRI consists of industry self-reported, facility-level chemical emissions that cause cancer or other chronic and/or acute adverse human health effects, as well as adverse environmental effects. RSEI uses the TRI emissions, along with toxicity information and population exposure modeling, to estimate the associated health hazards posed by emissions from each chemical at each facility.

We used the TRI to visualize the number of EtO-emitting facilities and their associated emissions over time within our study domain. Using RSEI hazard scores from air releases, we also calculated the total hazard attributable to each of four chemical classes (metals, non-VOC gases, non-EtO VOCs, and EtO) to understand the relative contributions to risk posed by facility chemical emissions in the sampling domain. Further details of how we accessed and processed these data are presented in the Supporting Information.

2.3.5. Risk Estimates from Measurements. As per the U.S. Environmental Protection Agency (EPA) Integrated Risk Information System (IRIS), the adult-based inhalation unit risk (IUR) for EtO is 3×10^{-3} per $\mu g\ m^{-3}$. The IUR quantifies the marginal upper-bound excess lifetime cancer risk resultant from a given exposure concentration and can be used to translate between exposure concentration and absolute levels of risk per eq 1:

$$R = \mathrm{IUR} \times \mathrm{EC} \tag{1}$$

where R is the risk level, IUR is the inhalation unit risk, and EC is the exposure concentration. Because EtO is known to be mutagenic, however, which implies increased susceptibility to cancer risk for early life exposure, we use the full lifetime IUR value of 5×10^{-3} per $\mu g\ m^{-3}$, where age-dependent adjustment factors (ADAFs) rescale the adult-based IUR, for translating all of our measured values into associated risks.

Relatedly, we report our measurement results as volume "mixing ratios," which are unit-less quantities (e.g., ppbv, pptv,

https://doi.org/10.1021/acs.est.3c10579
Environ. Sci. Technol. XXXX, XXX, XXX−XXX

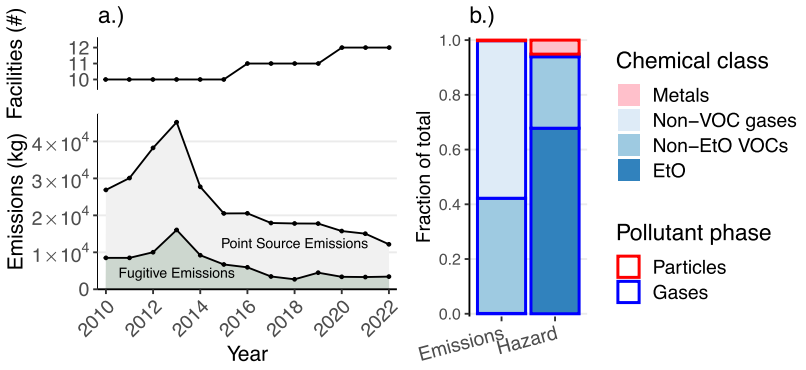

Figure 2. (a) Time series of the number of TRI-listed EtO-emitting facilities within the study domain (top panel), and the sum of TRI-listed fugitive and point source EtO emissions (bottom panel) within all Parishes highlighted in Figure 1a. (b) Year 2021 fractional contribution of each chemical category to total mass of hazardous air pollutant emissions (left bar) and total estimated RSEI hazard from all facilities in the larger corridor (right bar). The relative contribution of EtO by mass to total emissions is so low (~0.2%) that it is not visible in the "Emissions" bar of panel (b).

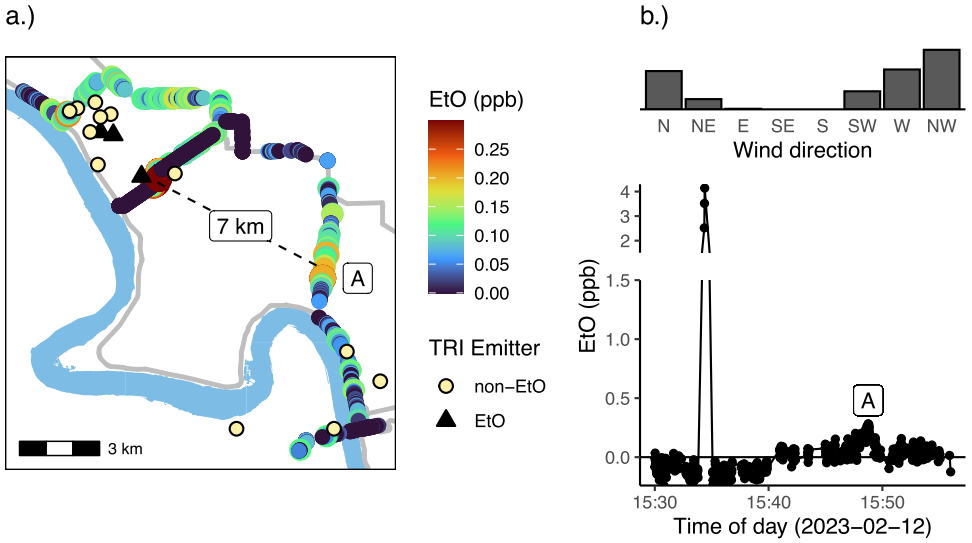

Figure 3. Map and time series of an intercepted plume from February 12. (a) Map shows where the AML intercepted a downwind plume (marked "A" on map). The likeliest emissions source is the EtO facility on the map near the other end of the dotted line. The map color scale is capped at 0.3 ppb to emphasize elevated EtO mixing ratios on the map in the vicinity of "A." Gray lines in the background show roads of the sampling route. (b) TILDAS EtO time series of data shown in map in panel (a), where the "A" marker on the time series corresponds to "A" on the map. The upper subpanel shows the measured wind direction during the same interval. We determined the likely source location based on WNW winds and a near-concurrent measurement of elevated EtO (~4 ppb plume) near the source.

abbreviated simply as "ppt" throughout) standard in gas-phase analytical chemistry. Mixing ratios literally refer to the number of molecules of interest per total number of molecules in air; each of the instruments used in this study report data as mixing ratios. While not technically correct, it is common across different fields of knowledge to use mixing ratio and "concentration" interchangeably, however. In this paper, "concentration" refers to mass concentration, which has units of e.g., $\mu g\ m^{-3}$, and is the fundamental exposure quantity in the context of IUR values. We relate mixing ratios to concentrations using the ideal gas law with an assumed pressure of 1 atm and temperature of 20 °C, which practically speaking has a unit conversion of 1 ppb = 1.83 $\mu g\ m^{-3}$.

3. RESULTS

3.1. TRI Emissions and RSEI Hazard for Facilities in the Sampling Domain. TRI-reported EtO emissions for facilities within the corridor decreased from 2010 to 2022, despite the total number of EtO-emitting facilities increasing from 10 to 12 (Figure 2a). The relative fraction of fugitive emissions to total (fugitive + point source) has also mostly decreased over this time period; in 2022, 27% of total emissions were fugitive, down from a high of 36% in 2013, though up from 22% in 2021. Year 2022 emissions were 1.2×10^4 kg, down from a peak of 4.5×10^4 kg in 2013.

EtO emissions represent less than 0.2% of total TRI emissions in the domain, using 2021 as an example year (Figure 2b). The majority (~57%) of 2021 TRI-reported emissions by mass are non-VOC gases (e.g., ammonia, hydrogen sulfide). Roughly 42% of 2021 TRI emissions are non-EtO VOCs, with the two largest contributors being hexane and ethylene (ethylene is the predominant precursor in the production of EtO[1]). Figure 2b shows the relative fraction of emissions and estimated hazards attributable to each category for 2021, though we found similar results across all years.

Due to its carcinogenicity per EPA IRIS, however, EtO contributes disproportionately to the total hazard associated

https://doi.org/10.1021/acs.est.3c10579
Environ. Sci. Technol. XXXX, XXX, XXX−XXX

with air emissions in the region. It represents ∼68% of the total hazard from air releases, which includes both cancer and noncancer risks, though it is almost exclusively due to cancer risk. The total hazard from the sum of all non-EtO VOCs is ∼26%, and that of metals is ∼5%.

3.2. Plume Analysis. We observed many EtO plumes during mobile sampling. Some were at the industrial fenceline of TRI-listed EtO emitters, while others were further afield. Using our plume characterization algorithm, we detected a total of 192 EtO plumes that both had maximum mixing ratios of 200 ppt or greater and lasted 10 s or longer. Of these, 90 (47%) of these plumes had mixing ratios exceeding 1 ppb, and the maximum plume mixing ratio we observed was 42.1 ppb (see Figure S6).

3.2.1. Spatial Extent of Plumes. Figure 3 shows an example plume, which we observed on February 12, 2023, and highlight here in order to illustrate the spatial extent of EtO plumes. We intercepted this plume in the Pelican Point residential community near Gonzalez in St. James Parish, 7 km downwind of its likely emission source. Figure 3a shows a map of the intercepted plume and its likely emissions source, and Figure 3b shows a time series plot of those same EtO mixing ratios. The wind direction during this period was largely from the WNW, and the wind speed ranged from 3 to 5 m s^{-1}.

The plume is marked "A" on the map, and the location most likely to be the emission source is traced from "A" with a dotted line. As indicated by the map, we observed high EtO mixing ratios in the close vicinity of the likely emissions source; these measurements were made roughly concurrently (within 10 min) with the observation of plume "A." Given the wind direction and concurrent even-higher EtO mixing ratios observed upwind of plume A, we conclude that the EtO-emitting facility near the end of the dotted line is the source, 7 km away.

We present similar figures for four other observed plumes in the Supporting Information (Figures S8−S11). These EtO plumes were measured between 1.3 and 11.4 km downwind of their likely sources, which establishes this range as the rough spatial extent of plume impacts that we observed in our sampling.

3.2.2. Wind Direction Analysis around Facility Cluster. The emission source shown in Figure 3a is part of a cluster of three EtO facilities that sit within a large industrial block in the northwestern part of the sampling area (labeled "facility cluster" in Figure 1b). We repeatedly saw high-concentration EtO plumes on these road sections over the course of mobile sampling.

Figure 4 shows all of the plumes identified in this area across the entire campaign that had a maximum EtO mixing ratio of at least 1 ppb and a duration of at least 10 s. We observed 50 distinct EtO plumes meeting the above criteria, which were spread relatively evenly across the duration of the campaign. While some were measured semiconcurrently (meaning within the same unique hour of sampling), we saw these plumes spread across 18 unique days and 34 unique hours of the campaign, indicating that emissions within the area were frequent across our month of sampling and not heavily biased toward, e.g., any day or two with much higher amounts of plume detection. Each panel corresponds to one of eight 45 degree wind direction bins; the map shows the location and relative size (by maximum mixing ratio) of EtO plumes observed when wind was blowing from the corresponding direction. Only plumes found within the highlighted polygon

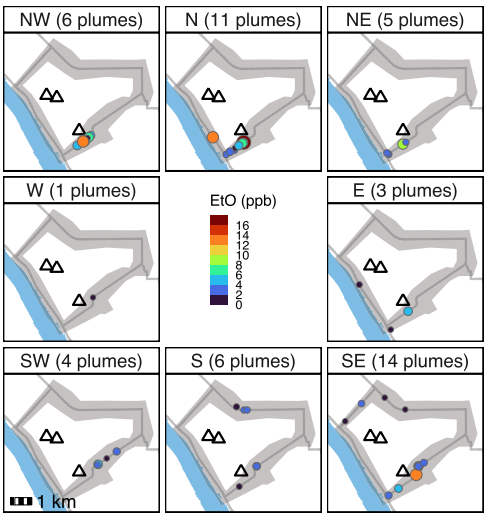

Figure 4. Plume locations around the dense facility cluster shown in Figure 1b. This area, bounded by the area highlighted by the light gray polygon on the map, contains three TRI-listed EtO emitters. We show plume locations within the area for different wind directions. Each plume is marked by its midpoint coordinates and is both colored and sized relative to its maximum EtO mixing ratio. EtO-emitting facilities are marked by a black "Δ." Dark gray lines in the background show roads of the sampling route.

are shown. TRI-listed EtO emitters are also marked on the map.

With winds from NW, N, or NE, we only saw plumes on the southern portion of the block. This suggests that on these roads, we are only measuring near-source EtO plumes from facilities within the block, as opposed to transported plumes from facilities further afield in the NW, N, or NE directions. If plumes were transported from outside of the block, we would expect to see them on the northern half, but we did not. Similarly, with winds from either E or W, we only saw plumes on the opposite side of the block (e.g., on the eastern side with winds from W, and vice versa). Winds from the SE, S, and SW directions presented a more complicated picture, as we saw plumes spread around multiple edges of the block, especially for SE and S winds. This likely indicates plumes transiting across the length of the block, where we detect them closer to their source at the SE portion of the block, and then on the opposite edges after transport at lower mixing ratios due to dispersion. This industrial block is clearly an important source of EtO, though pinpointing emissions to equipment or areas within facilities would require sampling within the fenceline (e.g., Thoma et al.[15]).

As demonstrated in the previous section, we observed EtO plumes ∼10 km away from this industrial block that very likely were emitted from facilities within. There are numerous residential areas and population centers within 10 km of this location as well, such as Carville, St. Gabriel, and Gonzalez.

3.2.3. Plume Categorization. Within EtO plumes, we analyzed the time series of other measured gas species in order to better understand the chemical mixtures present in EtO plumes, which provides information on potential sources. Three contrasting examples are shown in Figure S12, where the degree of correlation between EtO and each gas species is measured by R^2 for the in-plume portion of the time series. We see three different plume types for these examples: (1) EtO is uncorrelated with any other gas species, (2) EtO is correlated

https://doi.org/10.1021/acs.est.3c10579
Environ. Sci. Technol. XXXX, XXX, XXX−XXX

with a number of combustion-related species (e.g., CO_2, CO, NO_x) but not any natural gas-related species (e.g., CH_4 and C_2H_6), and (3) EtO other is highly correlated with both combustion-related species (e.g., CO_2) and some natural gas-related species (e.g., CH_4). We speculate that these three plumes represent emissions from (1) a pure EtO stream, such as direct emissions from storage or use; (2) an EtO process stream where other combustion products have not been removed; and (3) a flaring or thermal oxidizer scrubber waste stream where EtO is not being completely removed, respectively. Figure S13 summarizes the results of this analysis for a large number of plumes we observed, and more detail is provided in the Supporting Information. Fingerprinting EtO plumes by the presence or absence of other coemitted species will be required to better understand EtO emission sources in complex industrial environments like this one.

3.2.4. TILDAS–CRDS Comparison. Vehicle chase drives provided the opportunity to compare the two EtO instruments while measuring high-concentration EtO plumes. Figure 5a shows the time series of both instruments (TILDAS and CRDS) from a single pass near an EtO source by the two mobile laboratories. This illustrates how fast measurements are needed to detect facility plumes, especially from a mobile platform, as well as how the two instruments similarly capture the complex shape and magnitude of the plumes. There are observable differences in measurement noise when comparing the 1 s measurements. For the non-EtO plume portion of these passes (e.g., Figure 5a), the SD of the 1 Hz CRDS data is roughly ~9 × higher than the 1 Hz TILDAS data (630 ppt vs 70 ppt, respectively). This area had very high concentrations of methylene chloride, which can interfere with the CRDS measurement (see Supporting Information for further detail) and likely contribute to the measurement noise shown here. During other non-plume driving periods away from this location, 1 Hz CRDS SD was lower (~400 ppt).

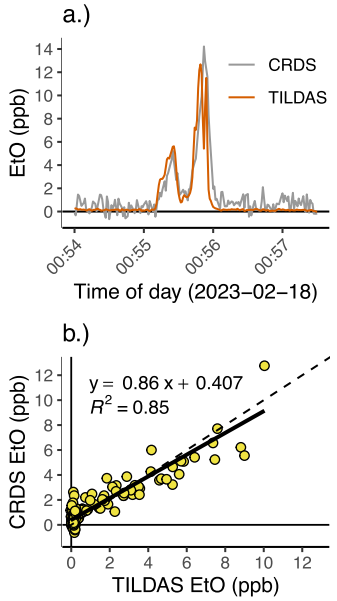

Figure 5. (a) Time series of each instrument for one example pass. (b) Correlation between CRDS and TILDAS for all four passes on 2023-02-18, where points used for the comparison are averaged over 15 s intervals to reduce noise. Dotted line is 1:1, and the solid line is the orthogonal distance regression fit to the data.

Figure 5b compares measurements between the two instruments for all four passes on 2022-02-18. The slope of the orthogonal distance regression using data from all four passes was 0.85, demonstrating that the TILDAS result tended to measure slightly higher than the CRDS. However, agreement within 20% is excellent for the purposes of plume detection and quantification, given that each instrument was aboard a separate vehicle, using a different inlet, and not measuring each plume truly simultaneously.

3.3. Spatially Resolved EtO Mixing Ratios. *3.3.1. By 500 m Grid Cell Aggregation.* Figure 6a shows average EtO mixing ratios across our sampling domain aggregated in 500 m grid cells (n = 428). The mean and median grid cell values were 31.4 and 23.3 ppt, respectively, and the 25th and 75th percentiles were 10.5 and 34.2 ppt, respectively.

At the northwestern and southeastern ends of the sampling domain, we see grid cell averages that are much higher than the median value. In the northwest, near Gonzalez, we see grid cell mixing ratios of 100 ppt and higher. As mentioned above, this area is dense with industrial sites: there are five EtO emitters encompassed by the driving route in this area and several others just outside of the route. Especially on roads around the facility cluster focused on in Section 3.2.2, we see elevated EtO levels. There is another EtO hotspot in the far northwest section of the domain around two EtO-emitting facilities. Similarly, in the southeastern part of the domain, we see grid cells with high EtO relative to the median grid cell values; this hotspot is also adjacent to an EtO-emitting facility.

3.3.2. By Land Use Category. Figure 6b illustrates how EtO mixing ratios vary between land-use categories related to facility proximity. We see clear differences, especially comparing grid cells that are not within 1 km of any facility ("None") to those within 1 km of an EtO-emitting facility ("EtO"). The "non-EtO" category has a slightly higher mean value than "None" (28.4 vs 22.1 ppt, respectively) and a handful of grid cells with high values. Given the density of industrial sites in this area, some of the "non-EtO" grid cells are physically close to "EtO" sites (i.e., just beyond the 1 km buffer we used) and likely are elevated due to emissions from these EtO facilities. This analysis shows very clearly that most of the highest grid cells in the domain are close to industrial sites, especially reported EtO emitters. These results were qualitatively similar when using larger buffer sizes (1.5 and 2 km) and are presented in the Supporting Information (Figure S15).

Across all land use categories, the associated risk values are considered high for a majority of grid cells. Mixing ratios corresponding to order-of-magnitude levels of chronic risk are indicated with horizontal lines in Figure 6b. A majority (n = 319, ~75%) of grid cells have mixing ratios larger than 10.9 ppt, which corresponds to 100-in-one-million risk (1×10^{-4}). Remediated EPA Superfund site projects, for reference, aim for a "target risk range"[41] between 1×10^{-6} and 1×10^{-4}. Risk levels above 1×10^{-4} are considered unacceptable by the EPA.[42]

There are also a number of grid cells (n = 14, ~3.3%) with values above 109 ppt, which corresponds to 1,000-in-one-million (1×10^{-3}) risk. Most of these grid cells are in near-source locations that are apart from residential areas. Still, they highlight a cause for concern for chronic occupational exposure at these facilities, as well as for any similar facilities in other locations where communities are located in very close proximity.

https://doi.org/10.1021/acs.est.3c10579
Environ. Sci. Technol. XXXX, XXX, XXX−XXX

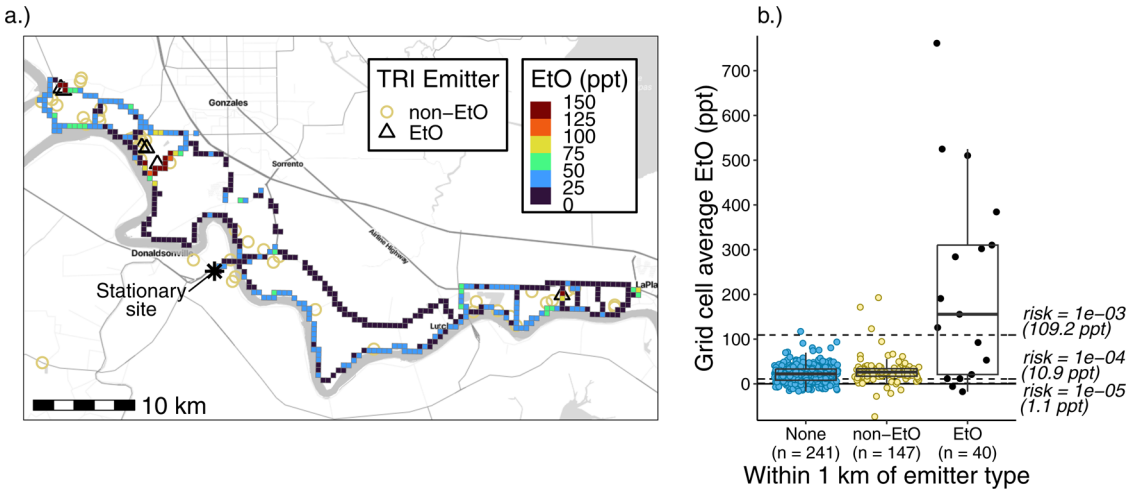

Figure 6. (a) EtO concentrations aggregated in 500 m grid cells from AML TILDAS measurements. All grid cells were visited 15 or more times. Facilities listed in the EPA TRI database are shown as well and colored by whether they report emitting EtO or not. (b) Box plots of grid cell average EtO concentrations for each of three land-use categories related to industrial facility proximity, with points representing individual grid cells. Horizontal lines and annotations on the right side of the plot show levels of cancer risk with corresponding lifetime EtO exposure concentrations.

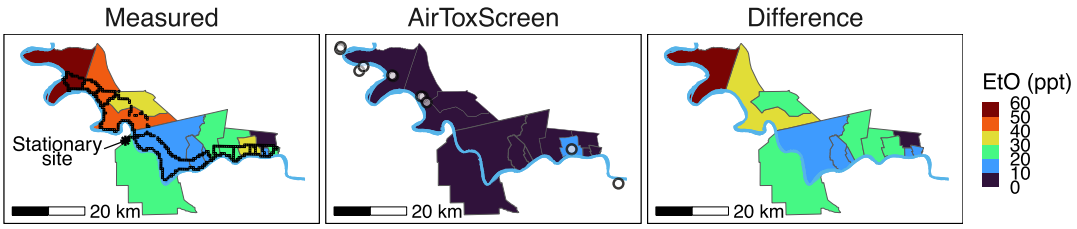

Figure 7. Census tract EtO values from measurements (left panel) and AirToxScreen (middle panel). The difference between measurements and AirToxScreen estimates is shown in the right panel. Stationary site and EtO-emitting facility locations are shown in the "Measured" and "Difference" panels, respectively, for reference. The grid cells we used to compute tract averages are overlaid in the "Measured" panel to give a sense for areal coverage within the grid cell.

3.3.3. By Census Tract. We made census tract-level EtO estimates by taking the mean of all grid cells within each of the 13 tracts in our domain (Figure 7). Our estimates range from 8.0 to 57.2 ppt, with the highest tract averages being those in the northwest of the domain. The median tract-level estimate from our measurements is 22.7 ppt.

These values exceed those estimated by 2019 AirToxScreen[29] for all tracts, which are shown in the middle panel of Figure 7. We visualize the difference between our tract-level estimates from measurements and those from AirToxScreen in the rightmost panel of Figure 7. The median tract-level mixing ratio for AirToxScreen estimates is 2.5 ppt, and the maximum tract estimate is 11.8 ppt. The highest tract concentration estimate for AirToxScreen is in the southeastern portion of the domain, as opposed to the northwestern portion of the domain, where our measurements are highest. The median difference is 21.3 ppt, and the maximum difference between tracts is 54.3 ppt.

All tract-level estimates from both our measurements and AirToxScreen are below 1000-in-one million (1×10^{-3}) levels of risk, though as shown in the previous section EtO can be highly spatially variable within a given tract. We estimate 12 of 13 tracts having EtO mixing ratios corresponding to 100- to 1000-in-one million levels of risk, with only one being between 10- and 100-in-one million. Only one of 13 AirToxScreen tracts are between 100- and 1000-in-one million levels of risk, with the other 12 being between 10- and 100-in-one million. Figure S14b shows a map of these risk estimates.

3.4. Stationary Site. The majority (80%) of measurements made by the EtO TILDAS instrument were made while the AML was at the stationary site. The mean and median EtO measured at the stationary site were 21.9 and 22.4 ppt, respectively. The median is similar to the median grid cell value from the "None" land use categories, which was 22.1 ppt. The SD for 1 Hz data at the stationary site was 84.4 ppt. For 1, 5, and 60 min averaging intervals, the SD was 68.3, 59.3, and 41.1 ppt, respectively.

Figure S17 shows the diurnal pattern of EtO measured at the stationary site. There is a slight mid-day increase in EtO, though the variation in hourly median values is small compared to the SD. The stationary site, which was 11.5 km southeast of the nearest EtO emitter, appears to be impacted by plumes from nearby facilities. We observed three short-duration (~3–120 s) plumes at the stationary site that had peak mixing ratios of ~1 ppb or higher; winds were NW for two of these three plumes and S for the other plume. During only ~9% of these measurements were winds from the NW, which would make the stationary site a potential receptor of emissions from the cluster of facilities discussed above. See Figure S18 for a wind rose for the stationary site measurements.

https://doi.org/10.1021/acs.est.3c10579
Environ. Sci. Technol. XXXX, XXX, XXX–XXX

4. DISCUSSION

It is noteworthy that across a region colloquially termed "Cancer Alley," a large majority (~68%, per Figure 2b) of the total facility-level air pollutant-related hazard is attributed solely to ethylene oxide, based on EPA RSEI estimates. We derived this figure from RSEI hazard scores, which are themselves derived from modeled concentrations based on emissions inventories built from industry self-reports; in short, these estimates are likely far from perfect. Nonetheless, the fact that so much of the environmental risk in this area seems to come from a single chemical is remarkable. This fact makes accurate and precise measurements of EtO near potential emission sources paramount for informing the environmental health concerns of nearby communities. With this novel data set, we report levels of EtO across space in an area densely populated with emitters and highlight important issues related to EtO measurements and associated impacts.

We identified EtO plumes up to 11.4 km away from likely sources based on wind direction analysis. While we did not find all grid cells within this distance from sources to be elevated above the mean EtO mixing ratio measured at the stationary site, the illustration of downwind plume intercepts gives a sense for which neighboring communities may be impacted by EtO emissions. For example, East Ascension High School near downtown Gonzales, LA, is approximately 8 km from the center of the industrial hotspot block discussed in Section 3.2.2. Though we did not conduct measurements in Gonzalez, it is one of a number of communities within the reach of potential EtO plume extents that could be candidates for longer-duration measurements. Ten kilometers is the distance used by the EPA to define "fenceline communities."[43] The spatial range of plume impacts could even be higher than the upper range that we observed; Yacovitch et al.[8] describe the potential transport of emissions from a source 35 km away.

We found a large majority of the domain to have EtO mixing ratios corresponding to risk levels above the EPA's acceptable upper limit (1×10^{-4}). A smaller number of locations in near-source areas had EtO levels corresponding to risk above 1×10^{-3}, representing potentially serious hazard for workers around these facilities.

The census tract-level comparison with AirToxScreen showed that AirToxScreen both substantially underestimates EtO across the entirety of the domain and fails to capture the spatial pattern identified by our measurements. There are no existing in-region EtO measurements to directly compare our data to or that could potentially be used for AirToxScreen model evaluation.[44] Thus, while these are the EPA's best estimates of tract-level EtO in the region, they lack ground-truthing by measurements and reflect the accuracy of the reported emissions. Given that the most up-to-date version of AirToxScreen is based on year 2019 emissions, we would expect an even larger discrepancy between our reported values and those estimated using AirToxScreen for the year 2023, as emissions decreased between 2019 and later years (see Figure 2). AirToxScreen ambient concentration estimates refer to annual, area-weighted census tract averages. We measured concentrations in February 2023 at a subset of locations within each tract. Below, we discuss whether these potential spatiotemporal sampling bias(es) might explain the large gap we see in concentrations (and thus estimated cancer risk) between measurements and this screening tool.

On potential temporal bias: any seasonality to the underlying emissions activity could potentially bias our measurements (higher or lower) relative to an annual average. Similarly, seasonal variation in EtO concentrations due to meteorological factors (e.g., typical planetary boundary layer heights or prevailing winds) could potentially bias our estimates (higher or lower) as well. For example, Yacovitch et al.[8] found slightly higher concentrations in the summer compared to the winter in Billerica, Massachusetts. However, as mentioned above, the reported emissions forming the basis of AirToxScreen estimates have decreased in recent years (31.5% decrease from 2019 to 2022), and would likely make the discrepancy even larger were the comparison against AirToxScreen estimates using year 2023 emissions; we speculate that this is more important than any potential seasonal bias, especially given that EtO is not formed from secondary chemistry. The declining trend in reported emissions also provides important context for thinking about lifelong exposures for residents in nearby communities; specifically, estimates of risk using contemporary measurements may underestimate true risks resulting from exposures at higher concentrations in previous years.

On potential spatial bias: AirToxScreen's spatial resolution is at tract-level, and so all parts of a tract are represented by a single ambient concentration. Our estimates, on the other hand, cover a subset of each tract and are necessarily limited to the roads we could drive on. We have tried to represent this potential bias by comparing the distribution of "distance-to-nearest" values between EtO-emitting facilities and each grid cell centroid, both for only those grid cells in which we made measurements and for the full set in a census tract. While there are differences in the distributions of this metric (see Figure S16), the bias appears minimal for those tracts with the highest EtO estimates from measurements, and so we think it is unlikely that this explains all or even much of the discrepancy we see between our estimates and AirToxScreen; in other words, our sampling reasonably represents the full span of the land use variable we expect to be most important for determining EtO concentrations across a tract. Unfortunately, a true area-weighted, tract-average estimate is impossible from a measurement perspective, given our inability to collect measurements on private property and the sparse road network in the area.

Lastly, we highlight our non-plume measurements in the context of what has been previously reported in the literature on EtO. There are currently a wide range of reported ambient background levels of EtO, which span a correspondingly wide range of associated cancer risk. Some, or perhaps even most, of this variability may be due to the analytical challenge of the measurement and artifacts associated with EtO determination using canister sampling and GC-MS, as highlighted by both EPA[22] and Hoisington and Herrington.[23] Despite the high density of TRI-listed EtO emitters in this domain, as well as the fact that we observed high-concentration plumes around each of them, the large majority (n = 356, ~83%) of grid cells in the domain still had sub-40 ppt mixing ratios. This is substantially lower than most of the urban background concentrations that have recently been reported from canister sampling with GC-MS analysis. For example, the average across 15 EPA Air Toxics sites reporting months-long EtO measurements, none of which are within 10 km of a TRI-listed EtO emitter, was 167 ppt, or over 7× higher than our stationary site average.[45] Spooner et al.[13] recently reported 24-

https://doi.org/10.1021/acs.est.3c10579
Environ. Sci. Technol. XXXX, XXX, XXX−XXX

h average concentrations at designated background sites (none within 15 km of the single TRI-listed emitter in the area) in greater Salt Lake City, UT that were 7−17× higher than our stationary site average. Similarly, Olaguer et al.[12] found 24h background concentrations in suburban Grand Rapids, MI ∼ 10× higher than our stationary site average. Our stationary site average concentration, as well as the median grid cell concentration from our mobile sampling, are much more comparable to those measurements reported from other *in situ* optical instruments by Yacovitch et al.[8] (Aerodyne TILDAS; suburban Boston, MA; ∼ 18 ppt) and Mei et al.[9] (Picarro CRDS; suburban Atlanta, GA; < 20 ppt). Given the high carcinogenicity of EtO (per EPA IRIS), ultraprecise and accurate measurements are needed to pinpoint risks posed to populations.

■ ASSOCIATED CONTENT

Supporting Information

The Supporting Information is available free of charge at https://pubs.acs.org/doi/10.1021/acs.est.3c10579.

Additional information regarding methods (calibrations, inlets, instrument operation, sampling route planning, and data processing) and results (plume spatial extents, plume characterization with other species, land use categorization buffer size, land use-related sampling bias, and stationary site EtO diurnal pattern) (PDF)

■ AUTHOR INFORMATION

Corresponding Author

Peter F. DeCarlo − *Department of Environmental Health and Engineering, Johns Hopkins University, Baltimore, Maryland 21218, United States;* orcid.org/0000-0001-6385-7149; Email: pdecarl1@jhu.edu

Authors

Ellis S. Robinson − *Department of Environmental Health and Engineering, Johns Hopkins University, Baltimore, Maryland 21218, United States;* orcid.org/0000-0003-1695-6392

Mina W. Tehrani − *Department of Environmental Health and Engineering, Johns Hopkins University, Baltimore, Maryland 21218, United States;* orcid.org/0000-0001-9946-7003

Amira Yassine − *Department of Environmental Health and Engineering, Johns Hopkins University, Baltimore, Maryland 21218, United States;* orcid.org/0000-0002-8692-6183

Shivang Agarwal − *Department of Environmental Health and Engineering, Johns Hopkins University, Baltimore, Maryland 21218, United States*

Benjamin A. Nault − *Department of Environmental Health and Engineering, Johns Hopkins University, Baltimore, Maryland 21218, United States; Center for Aerosol and Cloud Chemistry, Aerodyne Research, Inc., Billerica, Massachusetts 01821, United States;* orcid.org/0000-0001-9464-4787

Carolyn Gigot − *Department of Environmental Health and Engineering, Johns Hopkins University, Baltimore, Maryland 21218, United States;* orcid.org/0000-0002-0778-5539

Andrea A. Chiger − *Department of Environmental Health and Engineering, Johns Hopkins University, Baltimore, Maryland 21218, United States; The Risk Sciences and Public Policy Institute, Johns Hopkins Bloomberg School of Public Health, Baltimore, Maryland 21205, United States*

Sara N. Lupolt − *Department of Environmental Health and Engineering, Johns Hopkins University, Baltimore, Maryland 21218, United States; The Risk Sciences and Public Policy Institute, Johns Hopkins Bloomberg School of Public Health, Baltimore, Maryland 21205, United States;* orcid.org/0000-0001-6263-5333

Conner Daube − *Center for Atmospheric and Environmental Chemistry, Aerodyne Research, Inc., Billerica, Massachusetts 01821, United States*

Anita M. Avery − *Center for Aerosol and Cloud Chemistry, Aerodyne Research, Inc., Billerica, Massachusetts 01821, United States;* orcid.org/0000-0002-6130-9664

Megan S. Claflin − *Center for Aerosol and Cloud Chemistry, Aerodyne Research, Inc., Billerica, Massachusetts 01821, United States;* orcid.org/0000-0003-0878-8712

Harald Stark − *Center for Aerosol and Cloud Chemistry, Aerodyne Research, Inc., Billerica, Massachusetts 01821, United States; Department of Chemistry and Cooperative Institute for Research in Environmental Sciences, University of Colorado Boulder, Boulder, Colorado 80309, United States*

Elizabeth M. Lunny − *Center for Atmospheric and Environmental Chemistry, Aerodyne Research, Inc., Billerica, Massachusetts 01821, United States*

Joseph R. Roscioli − *Center for Atmospheric and Environmental Chemistry, Aerodyne Research, Inc., Billerica, Massachusetts 01821, United States*

Scott C. Herndon − *Center for Atmospheric and Environmental Chemistry, Aerodyne Research, Inc., Billerica, Massachusetts 01821, United States*

Kai Skog − *Picarro, Inc., Santa Clara, California 95054, United States*

Jonathan Bent − *Picarro, Inc., Santa Clara, California 95054, United States*

Kirsten Koehler − *Department of Environmental Health and Engineering, Johns Hopkins University, Baltimore, Maryland 21218, United States;* orcid.org/0000-0002-0516-6945

Ana M. Rule − *Department of Environmental Health and Engineering, Johns Hopkins University, Baltimore, Maryland 21218, United States;* orcid.org/0000-0003-2328-0749

Thomas Burke − *Department of Environmental Health and Engineering, Johns Hopkins University, Baltimore, Maryland 21218, United States; The Risk Sciences and Public Policy Institute, Johns Hopkins Bloomberg School of Public Health, Baltimore, Maryland 21205, United States;* orcid.org/0000-0003-4511-4792

Tara I. Yacovitch − *Center for Atmospheric and Environmental Chemistry, Aerodyne Research, Inc., Billerica, Massachusetts 01821, United States;* orcid.org/0000-0002-9604-116X

Keeve Nachman − *Department of Environmental Health and Engineering, Johns Hopkins University, Baltimore, Maryland 21218, United States; The Risk Sciences and Public Policy Institute, Johns Hopkins Bloomberg School of Public Health, Baltimore, Maryland 21205, United States*

Complete contact information is available at: https://pubs.acs.org/10.1021/acs.est.3c10579

Notes

The authors declare no competing financial interest.

https://doi.org/10.1021/acs.est.3c10579
Environ. Sci. Technol. XXXX, XXX, XXX−XXX

■ ACKNOWLEDGMENTS

This project was made possible through financial support from Bloomberg Philanthropies (Grant ID 2021-100480). P.F.D., K.K., A.M.R., and S.N.L. also received financial support from the National Institute of Environmental Health Sciences (NIEHS, Grant ID P30ES032756). K.K. received additional financial support from NIEHS (Grant ID P2CES033415). Local partners in southeastern Louisiana provided important guidance and connections that helped facilitate the project in many ways; these include Louisiana Bucket Brigade, Inclusive Louisiana, Tulane Environmental Law Clinic, and RISE St. James. We also thank all operators of the Aerodyne Mobile Laboratory who worked on in-field sampling and data analysis for this phase of HAP-MAP; these include Ben Werden, Ed Fortner, Kenji Lizardo, Ben Moul, Manjula Canagaratna, Zach Payne, and Tim Onasch.

■ REFERENCES

(1) Pu, T.; Tian, H.; Ford, M. E.; Rangarajan, S.; Wachs, I. E. Overview of Selective Oxidation of Ethylene to Ethylene Oxide by Ag Catalysts. *ACS Catal.* **2019**, *9*, 10727−10750.

(2) U.S. Environmental Protection Agency. *Evaluation of the Inhalation Carcinogenicity of Ethylene Oxide In Support of Summary Information on the Integrated Risk Information System (IRIS)*, 2016. https://cfpub.epa.gov/ncea/iris/iris_documents/documents/toxreviews/1025tr.pdf (accessed 2023-11-01).

(3) Texas Commission on Environmental Quality. *Ethylene Oxide Carcinogenic Dose-Response Assessment*, 2020. https://www.tceq.texas.gov/downloads/toxicology/dsd/final/eto.pdf; (accessed 2023-11-01).

(4) Sierra Club. *What Is TCEQ Hiding On Ethylene Oxide?*, 2021. https://www.sierraclub.org/texas/blog/2021/06/what-tceq-hiding-ethylene-oxide (accessed 2023-11-01).

(5) Sierra Club. *How Startup, Shutdown, and Malfunction Loopholes Give Free Passes to Polluters*, 2022. https://www.sierraclub.org/sites/www.sierraclub.org/files/2022-09/SSM_FactSheet.pdf (accessed 2023-11-01).

(6) U.S. Environmental Protection Agency. *Toxics Release Inventory (TRI) Program*. 2022. https://www.epa.gov/toxics-release-inventory-tri-program (accessed 2023-11-01).

(7) Galarneau, E.; Yacovitch, T. I.; Lerner, B.; Sheppard, A.; Quach, B.-T.; Kuang, W.; Rai, H.; Staebler, R.; Mihele, C.; Vogel, F. From hotspots to background: High-resolution mapping of ethylene oxide in urban air. *Atmos. Environ.* **2023**, *307*, No. 119828.

(8) Yacovitch, T. I.; Dyroff, C.; Roscioli, J. R.; Daube, C.; McManus, J. B.; Herndon, S. C. Ethylene oxide monitor with part-per-trillion precision for *in situ* measurements. *Atmospheric Measurement Techniques* **2023**, *16*, 1915−1921.

(9) Mei, E. J.; Moore, A. C.; Kaiser, J. Suitability of new and existing ambient ethylene oxide measurement techniques for cancer inhalation risk assessment. *Environ. Pollut.* **2023**, *336*, No. 122481.

(10) Sheehan, P. J.; Lewis, R. C.; Kirman, C. R.; Watson, H. N.; Winegar, E. D.; Bus, J. S. Ethylene Oxide Exposure in U.S. Populations Residing Near Sterilization and Other Industrial Facilities: Context Based on Endogenous and Total Equivalent Concentration Exposures. *International Journal of Environmental Research and Public Health* **2021**, *18*, 607.

(11) Lewis, R. C.; Sheehan, P. J.; DesAutels, C. G.; Watson, H. N.; Kirman, C. R. Monitored and Modeled Ambient Air Concentrations of Ethylene Oxide: Contextualizing Health Risk for Potentially Exposed Populations in Georgia. *International Journal of Environmental Research and Public Health* **2022**, *19*, 3364.

(12) Olaguer, E. P.; Robinson, A.; Kilmer, S.; Haywood, J.; Lehner, D. Ethylene Oxide Exposure Attribution and Emissions Quantification Based on Ambient Air Measurements near a Sterilization Facility. *International Journal of Environmental Research and Public Health* **2020**, *17*, 42.

(13) Spooner, S.; Handy, R.; Daher, N.; Edie, R.; Henry, T.; Sleeth, D. A Comparison of Ambient Air Ethylene Oxide Modeling Estimates from Facility Stack and Fugitive Emissions to Canister-based Ambient Air Measurements in the Salt Lake City. *Air* **2023**, *1*, 175−183, DOI: 10.3390/air1030013.

(14) Vazquez, S. No Consensus: Patchwork Remedies and the Health Crisis Linked to Ethylene Oxide Medical Sterilization Facilities. *Northern Illinois Univ. Law Rev.* **2021**, *41*, 1−28.

(15) Thoma, E. D.; Gitipour, A.; George, I.; Kariher, P.; MacDonald, M.; Queiroz, G.; Deshmukh, P.; Childers, J.; Rodak, T.; Schmid, V. Assessment of chemical facility ethylene oxide emissions using mobile and multipoint monitoring. *Atmospheric Environment: X* **2023**, *18*, No. 100214.

(16) U.S. Environmental Protection Agency. *Community Engagement on Ethylene Oxide (EtO)*, 2022. https://www.epa.gov/hazardous-air-pollutants-ethylene-oxide/forms/community-engagement-ethylene-oxide-eto (accessed 2023-11-01).

(17) Friedman, L. *In 'Cancer Alley,' Judge Blocks Huge Petrochemical Plant*; The New York Times: 2022. https://www.nytimes.com/2022/09/15/climate/louisiana-judge-blocks-formosa-plant.html (accessed 2023-11-01).

(18) Blodgett, A. D. An Analysis of Pollution and Community Advocacy in 'Cancer Alley': Setting an Example for the Environmental Justice Movement in St James Parish, Louisiana. *Local Environment* **2006**, *11*, 647−661.

(19) Terrell, K. A.; Julien, G. S. Air pollution is linked to higher cancer rates among black or impoverished communities in Louisiana. *Environ. Res. Lett.* **2022**, *17*, No. 014033.

(20) Galarneau, E.; Wang, D.; Dabek-Zlotorzynska, E.; Siu, M.; Celo, V.; Tardif, M.; Harnish, D.; Jiang, Y. Air toxics in Canada measured by the National Air Pollution Surveillance (NAPS) program and their relation to ambient air quality guidelines. *J. Air Waste Manage. Assoc.* **2016**, *66*, 184−200.

(21) U.S. Environmental Protection Agency. *Addendum to "Draft Human Health and Ecological Risk Assessment in Support of Registration Review" - Inhalation Exposure Risk Assessment in Support of Registration Review*, 2023. https://www.epa.gov/system/files/documents/2023-04/eto-draft-human-healh-ra-add.pdf (accessed 2023-11-01).

(22) Phelps, L., *Memorandum: Effect of Canister Type on Background Ethylene Oxide Concentrations*; U.S. Environmental Protection Agency: 2021. https://www.epa.gov/sites/default/files/2021-05/documents/ord-eto-canister-background-memo-05072021.pdf (accessed 2023-11-01).

(23) Hoisington, J.; Herrington, J. S. Rapid Determination of Ethylene Oxide and 75 VOCs in Ambient Air with Canister Sampling and Associated Growth Issues. *Separations* **2021**, *8*, 35.

(24) Lucic, G.; Rella, C.; Hoffnagle, J.; Skog, K.; McHale, L. Novel, real-time measurements of VOCs using a Cavity Ring-Down Spectrometer (CRDS). In *EGU General Assembly 2020 (Online)*; 2020 (accessed 2023-11-01).

(25) Gupta, M.; Chan, A. P.; Sullivan, M. N.; Gupta, R. M. Trace Measurements of Ethylene Oxide Using Cavity-enhanced Absorption Spectrometry near 3066 cm−1. *Aerosol and Air Quality Research* **2022**, *22*, No. 220046.

(26) Wang, A.; Paul, S.; deSouza, P.; Machida, Y.; Mora, S.; Duarte, F.; Ratti, C. Key Themes, Trends, and Drivers of Mobile Ambient Air Quality Monitoring: A Systematic Review and Meta-Analysis. *Environ. Sci. Technol.* **2023**, *57*, 9427−9444.

(27) Yacovitch, T. I.; Herndon, S. C.; Roscioli, J. R.; Floerchinger, C.; Knighton, W. B.; Kolb, C. E. Air Pollutant Mapping with a Mobile Laboratory during the BEE-TEX Field Study. *Environ. Health Insights* **2015**, *9s4* (Suppl 4), 7.

(28) Yacovitch, T. I.; Lerner, B. M.; Canagaratna, M. R.; Daube, C.; Healy, R. M.; Wang, J. M.; Fortner, E. C.; Majluf, F.; Claflin, M. S.; Roscioli, J. R.; Lunny, E. M.; Herndon, S. C. Mobile Laboratory Investigations of Industrial Point Source Emissions during the MOOSE Field Campaign. *Atmosphere* **2023**, *14*, 1632.

(29) U.S. Environmental Protection Agency. *2019 Air Toxics Screening Assessment*, 2022. https://www.epa.gov/AirToxScreen/2019-airtoxscreen; (accessed 2023-11-01).
(30) Herndon, S. C.; Jayne, J. T.; Zahniser, M. S.; Worsnop, D. R.; Knighton, B.; Alwine, E.; Lamb, B. K.; Zavala, M.; Nelson, D. D.; McManus, J. B.; Shorter, J. H.; Canagaratna, M. R.; Onasch, T. B.; Kolb, C. E. Characterization of urban pollutant emission fluxes and ambient concentration distributions using a mobile laboratory with rapid response instrumentation. *Faraday Discuss.* **2005**, *130*, 327−339.
(31) Yacovitch, T. I.; Herndon, S. C.; Petron, G.; Kofler, J.; Lyon, D.; Zahniser, M. S.; Kolb, C. E. Mobile Laboratory Observations of Methane Emissions in the Barnett Shale Region. *Environ. Sci. Technol.* **2015**, *49*, 7889−7895.
(32) Apte, J. S.; Messier, K. P.; Gani, S.; Brauer, M.; Kirchstetter, T. W.; Lunden, M. M.; Marshall, J. D.; Portier, C. J.; Vermeulen, R. C.; Hamburg, S. P. High-Resolution Air Pollution Mapping with Google Street View Cars: Exploiting Big Data. *Environ. Sci. Technol.* **2017**, *51*, 6999−7008.
(33) Targino, A. C.; Oliveira, M. V. B.; Krecl, P. Ubiquity of hazardous airborne substances on passenger ferries. *Journal of Hazardous Materials* **2022**, *423*, No. 127133.
(34) Robinson, E. S.; Cesler-Maloney, M.; Tan, X.; Mao, J.; Simpson, W.; DeCarlo, P. F. Wintertime spatial patterns of particulate matter in Fairbanks, AK during ALPACA 2022. *Environmental Science: Atmospheres* **2023**, *3*, 568−580.
(35) Pebesma, E. Simple Features for R: Standardized Support for Spatial Vector Data. *R Journal* **2018**, *10*, 439.
(36) Carslaw, D. C.; Ropkins, K. openair — An R package for air quality data analysis. *Environmental Modelling & Software* **2012**, *27*, 52−61.
(37) Kahle, D.; Wickham, H. ggmap: Spatial Visualization with ggplot2. *R Journal* **2013**, *5*, 144.
(38) Actkinson, B.; Ensor, K.; Griffin, R. J. SIBaR: a new method for background quantification and removal from mobile air pollution measurements. *Atmospheric Measurement Techniques* **2021**, *14*, 5809−5821.
(39) Goetz, J. D.; Avery, A.; Werden, B.; Floerchinger, C.; Fortner, E. C.; Wormhoudt, J.; Massoli, P.; Herndon, S. C.; Kolb, C. E.; Knighton, W. B.; Peischl, J.; Warneke, C.; Gouw, J. A. D.; Shaw, S. L.; DeCarlo, P. F. Analysis of local-scale background concentrations of methane and other gas-phase species in the Marcellus Shale. *Elem.: Sci. Anthropocene* **2017**, *5*, 1.
(40) U.S. Environmental Protection Agency. *Risk-Screening Environmental Indicators (RSEI) Model*, 2022. https://www.epa.gov/rsei (accessed 2023-11-01).
(41) Clay, D. *Memorandum: Role of the Baseline Risk Assessment in Superfund Remedy Selection Decisions*; U.S. Environmental Protection Agency; 1991. https://www.epa.gov/sites/default/files/2015-11/documents/baseline.pdf (accessed 2023-11-01).
(42) U.S. Environmental Protection Agency. *Report No. 21-P-0129: EPA Should Conduct New Residual Risk and Technology Reviews for Chloroprene and Ethylene Oxide-Emitting Source Categories to Protect Human Health*, 2021. https://www.epaoig.gov/sites/default/files/2021-05/documents/_epaoig_20210506-21-p-0129.pdf (accessed 2023-11-01).
(43) U.S. Environmental Protection Agency. *Draft TSCA Screening Level Approach for Assessing Ambient Air and Water Exposures to Fenceline Communities Version 1.0*, 2022. https://www.epa.gov/system/files/documents/2022-01/draft-fenceline-report_sacc.pdf (accessed 2023-11-01).
(44) U.S. Environmental Protection Agency. *AMTIC - Ambient Monitoring Archive for HAPs*, 2023. https://www.epa.gov/amtic/amtic-ambient-monitoring-archive-haps (accessed 2023-11-01).
(45) U.S. Environmental Protection Agency. *Ethylene Oxide Ambient Concentrations at National Air Toxics Trends Stations and Urban Air Toxics Monitoring Program stations October 1, 2018 − March 31, 2019*, 2022. https://www.epa.gov/sites/default/files/2019-11/documents/data_summary_stations.pdf (accessed 2023-11-01).

https://doi.org/10.1021/acs.est.3c10579
Environ. Sci. Technol. XXXX, XXX, XXX−XXX